PRECEDING PAGE BLANK NOT FILMED.   TG # 27

LUNAR SURFACE ROUGHNESS
SHADOWING AND THERMAL EMISSION

B. G. Smith

August, 1966

Contract No. NSR-24-005-047

Prepared by

UNIVERSITY OF MINNESOTA

Minneapolis, Minnesota

For

HEADQUARTERS, NATIONAL AERONAUTICS & SPACE ADMINISTRATION

Washington, D. C. 20546

LUNAR SURFACE ROUGHNESS, SHADOWING AND THERMAL EMISSION

ABSTRACT

A statistical model of surface roughness is used in an attempt to understand the gross infrared emissive characteristics of the Moon. A self-shadowing theory of rough surfaces is developed which is relevant also, in a different context, to the determination of mean surface slope from shadow measurements, a technique of use in the analysis of Lunar Orbiter photographs.

TABLE OF CONTENTS

LIST OF ILLUSTRATIONS

LUNAR SURFACE ROUGHNESS, SHADOWING AND THERMAL EMISSION

B. G. Smith

August, 1966

INTRODUCTION

The surface of the Moon is rough, both microscopically as deduced from photometric studies (ref. 1) and on the large scale as observed through telescopes, and various theoretical models have been constructed to incorporate the effect of surface roughness in the interpretation of lunar remote sensing experiments. A statistical description of the surface in terms of a density distribution of height deviations from a mean spherical Moon has been particularly useful in an understanding of the lunar radar backscattering properties (ref. 2) and an attempt is made in this paper to extend the use of the statistical model to examine the effect of surface roughness on the overall emission of thermal radiation and the casting of shadows in sunlight.

The model describes the Moon as a smooth sphere upon which are superimposed positive and negative undulations of height generated by a stationary random process.* Locally the underlying surface may be considered plane. The density distribution of surface height deviations (ξ) from the mean surface is described by a continuous probability function $P(\xi)$, of zero mean, chosen to be Gaussian for computational ease, where the probability of finding a

---

*It is likely that the surface is in fact composite, being a superimposition of roughness of several different scales. It will be assumed that any experiment is particularly sensitive to one scale.

height deviation within the range $\Delta\xi$ about ξ is

$$P(\xi)\,\Delta\xi \;=\; \frac{1}{(2\pi)^{1/2}\,\sigma}\; e^{-\xi^2/2\sigma^2} \cdot \Delta\xi \tag{1}$$

and σ is the root mean square height deviation. The horizontal scale of the relief is contained within an autocorrelation function $\rho(r)$, defined by

$$\rho(r) \;=\; \left\langle \xi(\underline{x} + \underline{r})\,\xi(\underline{x}) \right\rangle \tag{2}$$

the average being taken over all vectors $\underline{x}$ lying in the mean plane. $\rho(r)$ is independent of the direction of $\underline{r}$ for an isotropic surface. Higher dimensional distribution functions and their appropriate correlation matrices may be derived from the autocorrelation function $\rho(r)$ (ref. 3). In particular, the joint distribution function of surface slopes $p\ \left(=\dfrac{\partial\xi}{\partial x}\right)$ and $q\ \left(= \partial\xi/\partial y\right)$ for the Gaussian surface described by (1) is:

$$P(p,q) \;=\; \frac{1}{2\pi w^2}\; e^{-\frac{p^2+q^2}{2w^2}} \tag{3}$$

where w^2, the mean square surface slope is $\left[\dfrac{d^2}{dr^2}\,\rho(r)\right]_{r\,=\,0}$.

Each infinitesimal element of the surface can absorb, reflect and emit radiation, and possibly shadow its fellows, and the behavior of the surface as a whole is the summation of elemental contributions.

2

SHADOWING THEORY

Geometrical self-shadowing of the surface presents the greatest analytical difficulty and will be discussed first, with an approach essentially similar to that used in a recent paper by Wagner (ref. 4), suggested by Beckmann (ref. 5). The problem is the following: What is the probability $S(\xi, p, q, \theta)$ that a point A on a random rough surface, of given height ξ above the mean plane and with local slopes p, q will not lie in shadow when the surface is illuminated with a parallel beam of radiation at an angle of incidence θ to the mean plane? Figure 1 illustrates a section through the surface. The origin of coordinates is taken in the mean plane below A and the axes oriented with the incoming beam lying in the x=o plane. Only parts of the surface in this plane to the right of A can shadow A, and $S(\xi, p, q, \theta)$ or $S(A, \theta)$ for short, is equivalent to the probability that no part of the surface to the right of A will intersect the ray AS. This, in turn, may be written as the limit:

$$S(A, \theta) = \lim_{\tau \to \infty} S(A, \theta, \tau) \tag{4}$$

where $S(A, \theta, \tau)$ is the probability that no part of the surface between y=o and y=τ will intersect the ray AS. A differential equation for $S(A, \theta, \tau)$ may be developed thus:

$$S(A, \theta, \tau + \Delta\tau) = S(A, \theta, \tau) \cdot Q(A, \theta, \tau \mid \Delta\tau) \tag{5}$$

where now $Q(A, \theta, \tau \mid \Delta\tau)$ is the conditional probability that the surface will not intersect AS in the interval $\Delta\tau$ given that it does not in the interval τ. Turning this around and suppressing the functional dependence upon A, θ:

$$Q(A, \theta, \tau \mid \Delta\tau) = 1 - g(\tau) \Delta\tau \tag{6}$$
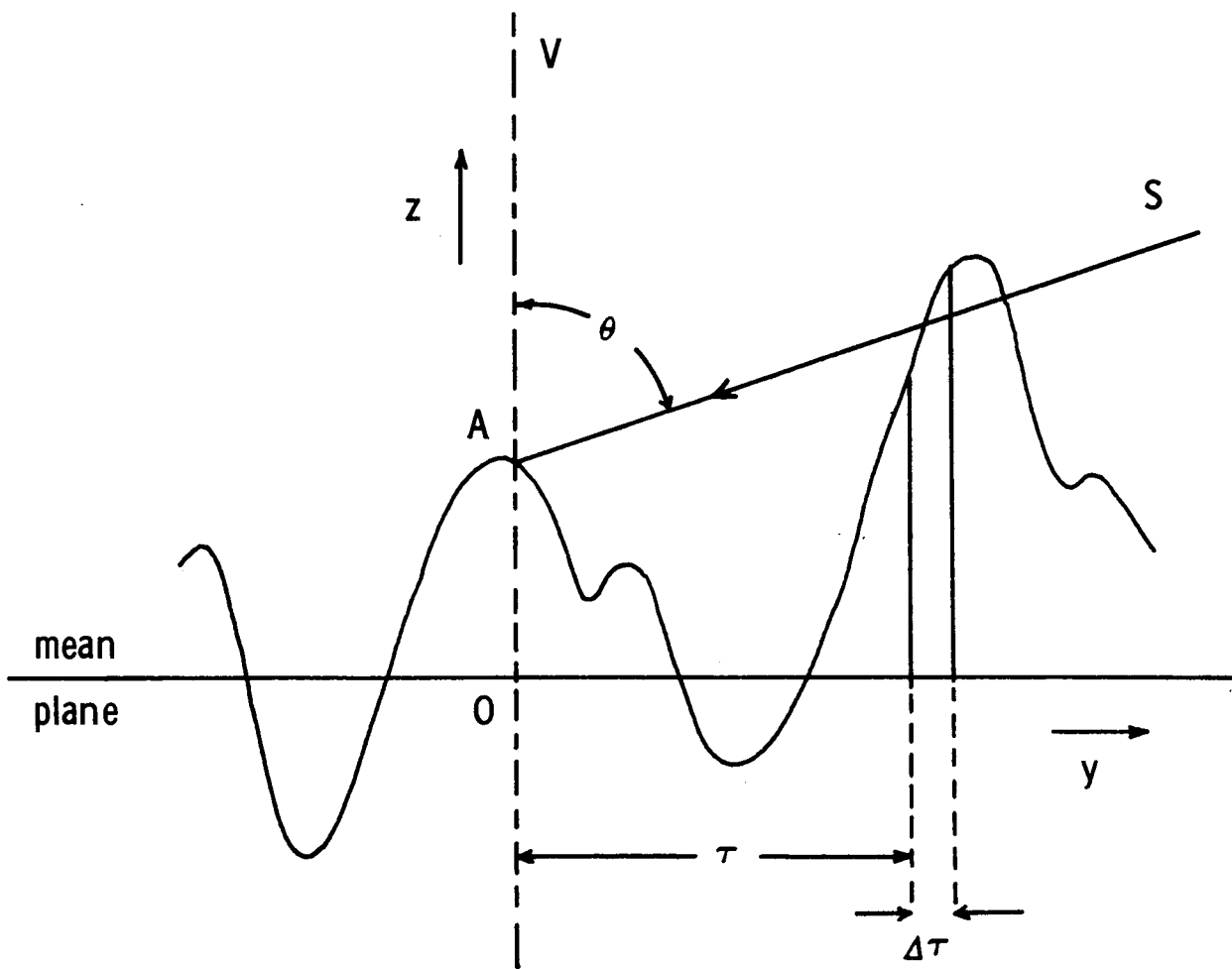
Figure 1: Section of a random rough surface illuminated from S

where $g(\tau) \Delta\tau$ is the conditional probability that the surface in $\Delta\tau$ will intersect the ray AS given that it does not in the interval τ. Equation (5) now becomes, again suppressing explicit A and θ dependence:

$$S(\tau + \Delta\tau) = S(\tau) \cdot \left\{ 1 - g(\tau) \Delta\tau \right\} \tag{7}$$

Expanding $S(\tau + \Delta\tau)$ about τ in a Taylor Series to first order in $\Delta\tau$ leads to the differential equation

$$\frac{dS(\tau)}{d\tau} = - g(\tau) \cdot S(\tau) \tag{8}$$

which may be integrated to yield

$$S(\tau) = S(o) \exp \left\{ - \int_0^\tau g(\tau) d\tau \right\} \tag{9}$$

$S(o)$ will clearly be unity if q is less than cot θ and zero otherwise, so $S(o) = h(u, q)$, where h is the unit step function and $\mu = \cot\theta$. Equation (4) now becomes

$$S(A, \theta) = h(\mu - q) \exp \left\{ - \int_0^\infty g(\tau) d\tau \right\} \tag{10}$$

The heart of the task lies in the evaluation of $g(\tau)$ and the subsequent integration over τ. Instead of an attempt at a complete analysis $g(\tau)$ will be approximated by replacing $g(\tau) \Delta\tau$ with the conditonal probability that A will be shadowed by the surface in $\Delta\tau$ given that it is not shadowed by the surface at $y=\tau$. (This avoids the difficulty of including the effects of correlation between points on the surface in $\Delta\tau$ and the infinity of points in τ).

If the surface at τ does not shadow A,

$$z(\tau) < \xi + \mu\tau \qquad (11)$$

symbolically denoted as circumstance α.

If the surface in $\Delta\tau$ does shadow A, and $\eta = \left(\dfrac{\partial z}{\partial y}\right)_{y=\tau}$,

$$z(\tau) < \xi + \mu\tau; \quad z(\tau + \Delta\tau) > \xi + \mu.(\tau + \Delta\tau); \quad \eta \geq \mu \qquad (12)$$

that is: $z(\tau)$ must lie in the interval $(\eta - \mu)\Delta\tau$ below $\xi + \mu\tau$, and $\eta \geq \mu$, denoted as circumstance β. $g(\tau)\Delta\tau$ is just the conditional probability that β will occur given α, or

$$g(\tau)\Delta\tau = R(\beta \mid \alpha) \qquad (13)$$

A well known relationship in probability theory links $R(\beta \mid \alpha)$ with $R(\alpha, \beta)$ and $R(\alpha)$, respectively the probability of α and β occurring independently and the probability of α occurring by itself:

$$R(\alpha, \beta) = R(\beta \mid \alpha) . R(\alpha) \qquad (14)$$

therefore

$$g(\tau)\Delta\tau = \frac{R(\alpha, \beta)}{R(\alpha)} \qquad (15)$$

If $P(z, \eta \mid A, \tau)$ is the joint probability distribution function of z and η at $y = \tau$ conditonal upon given height and slopes at A, then from the meaning of circumstances α and β, equations (11, 12)

$$R(\alpha, \beta) = \Delta\tau \int_{\mu}^{\infty} d\eta \, (\eta - \mu) \left[P(z, \eta \, A, \tau) \right]_{z \, = \, \xi \, + \mu\tau} \tag{16}$$

and

$$R(\alpha) = \int_{-\infty}^{+\infty} d\eta \int_{-\infty}^{\xi+\mu\tau} dz \, P(z, \eta \mid A, \tau) \tag{17}$$

and so

$$g(\tau) \, \Delta\tau = \frac{\Delta\tau \int_{\mu}^{\infty} d\eta (\eta-\mu) \left[P(z, \eta \mid A, \tau) \right]_{z \, = \, \xi \, + \mu\tau}}{\int_{-\infty}^{+\infty} d\eta \int_{-\infty}^{\xi+\mu\tau} dz \, P(z, \eta \mid A, \tau)} \tag{18}$$

where the renormalization effected by the denominator allows for the condition that $z(\tau)$ is known to be $\leq \xi + \mu\tau$.

With known distribution and auto-correlation functions the integrals in equation (18) may be evaluated in full, but this is a tedious process and not illuminating. Great simplicity is gained by neglecting correlation between the height and slopes at A and those at $y = \tau$. The conditional distribution function in this case reduces to a product of Gaussian functions:

$$P(z, \eta \, A, \tau) = P(z) \, P(\eta) = \frac{1}{2\pi \sigma w} \, e^{-z^2/2\sigma^2 - \eta^2/2w^2} \tag{19}$$

and within this approximation equation (18) becomes

7

$$g(\tau) = \frac{\mu(2\pi)^{1/2} \wedge(\mu) \cdot e^{\frac{(\xi + \mu\tau)^2}{2\sigma^2}}}{\sigma \left[2 - \text{erfc} \left(\frac{\xi + \mu\tau}{\sqrt{2}\sigma} \right) \right]} \tag{20}$$

where erfc is the error function complement and

$$2\wedge(\mu) = \left[\left(\frac{2}{\pi} \right)^{1/2} \cdot \frac{w}{\mu} e^{-\mu^2/2w^2} - \text{erfc} \left(\mu/\sqrt{2}w \right) \right] \tag{21}$$

The integration over τ (equation (10) is now simple and leads to

$$S(A, \theta) = S(\xi, p, q, \theta) = h(\mu - q) \left[1 - 1/2 \, \text{erfc} \left(\xi/\sqrt{2}\sigma \right) \right]^{\wedge} \tag{22}$$

Two further distributions may be deduced from $S(A, \theta)$: the probability of A not being shadowed, independent of ξ which is

$$S(p, q, \theta) = \int_{-\infty}^{+\infty} S(\xi, p, q, \theta) \, P(\xi) \, d\xi = \frac{h(\mu - q)}{\left[\wedge(\mu) + 1 \right]} \tag{23}$$

and the probability that a point on the surface will not be shadowed, independent of height and slope, $S(\theta)$

$$S(\theta) = \int_{-\infty}^{+\infty} d\xi \int_{-\infty}^{+\infty} dp \int_{-\infty}^{+\infty} dq \, P(\xi) \, P(p) \, P(q) \, S(\xi, p, q, \theta)$$

$$= \frac{\left[1 - 1/2 \, \text{erfc}(\mu/\sqrt{2}w \right]}{\left[\wedge(\mu) + 1 \right]} \tag{24}$$

The expression for $S(\theta)$ is compared in Figure 2 with that derived by Brockelman and Hagfors (ref. 6) from a computer simulation of an illuminated Gaussian random rough surface; good agreement is achieved between present theory and 'experiment'. Wagner (ref. 4) does not use the device of renormalization, equation (18), and instead includes correlation directly in the form of a Gaussian autocorrelation function to evaluate the conditional probability function $P(z, \eta \mid A, \tau)$. He is forced to approximate the integral over τ, equation (10), and at the expense of analytical complexity in fact gains a closer agreement with the simulation. Equation (24) provides an adequate approximation for the present purpose, and as will be seen later contains an advantage in satisfying a self-consistency condition. Recalling the salient result of shadowing theory which will be needed subsequently: the probability that a point on the surface with local slopes p, q will be illuminated by a beam of incidence angle θ is

$$S(p, q, \theta) = \frac{h(\mu - q)}{\left[\wedge(\mu) + 1\right]} = S(q, \theta) \quad \text{(independent of p)} \tag{25}$$

OPTICAL SHADOWING

A measurement of the fraction of a rough surface visibly illuminated yields $S(\theta)$ directly and would provide an experimental means of investigating the statistical parameters of the surface; in the case of a Gaussian surface it would allow a determination of the mean slope. To explain the method shadowing theory must be developed further. Figure 3 illustrates a section of a two dimensional surface illuminated from the right. δA is a surface element at P with local normal PN; PV is normal to the mean plane and PS is the illuminating ray. PK is the direction to a distant observer, and for simplicity it will be assumed that PK lies in the plane of illumination, defined as that plane containing PV and PS. The visibly illuminated area of the whole
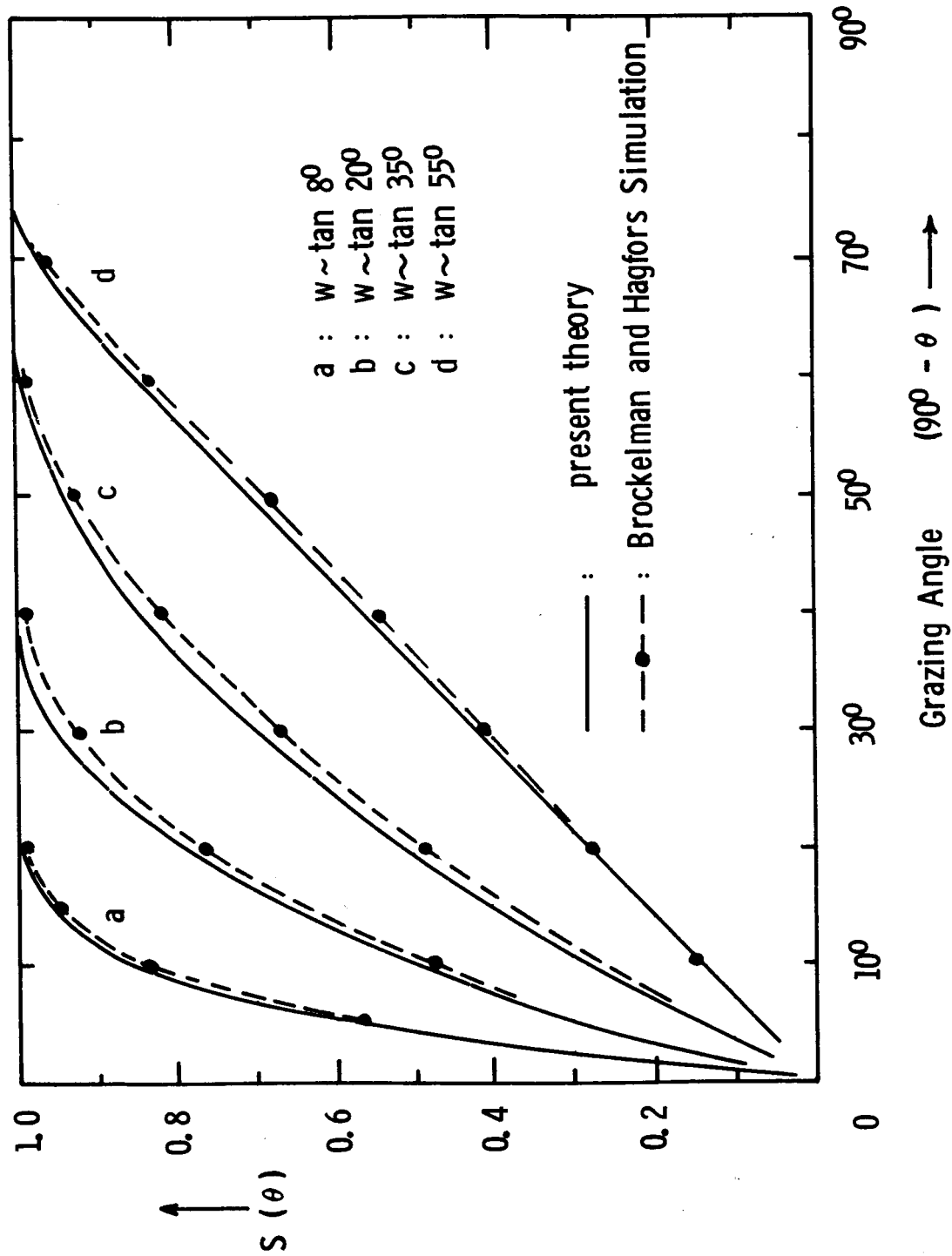
Figure 2: Comparison of the theoretical shadowing function S (θ) with the simulation of Brockelman and Hagfors
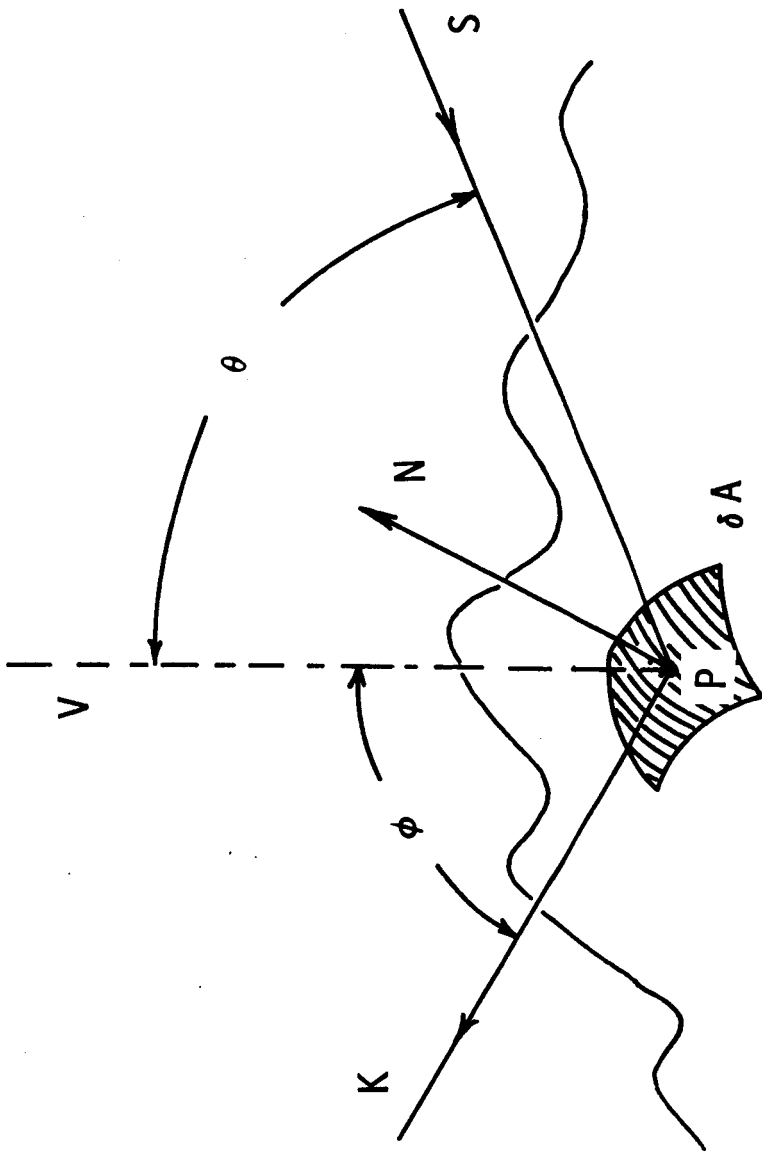
Figure 3: Part of a random rough surface illuminated from S and observed from K

surface projected onto the plane perpendicular to the direction of view is

$$\iint\limits_{\text{surface}} dA\, J(p, q, \theta, \varphi)\, \cos\, K\hat{P}N = \iint\limits_{\substack{\text{area } A_0 \text{ in} \\ \text{xy plane}}} dxdy\, J(p, q, \theta, \varphi)\frac{\cos\, K\hat{P}N}{\cos\, V\hat{P}N}$$

(26)

where J is a function having the value unity if δA can be seen to be illuminated and zero otherwise. Integration over the surface is equivalent to taking an average over the distribution of illuminated facets (invoking the ergodic theorem) and so:

$$\begin{matrix}\text{projected} \\ \text{illuminated area}\end{matrix} = A_0 \iint dpdq\, P(p)\, P(q)\, T(p, q, \theta, \varphi)\frac{\cos\, K\hat{P}N}{\cos\, V\hat{P}N}$$

$$= fA_0 \cos \varphi$$

(27)

where f is the fraction of the total projected area illuminated and $T(p, q, \theta, \varphi)$ is the probability that a point with slopes p, q will not be shadowed for either of the ray directions PS or PK. It is necessary to consider three distinct ranges of φ, and the sign convention will be used in which angles measured toward the source of illumination are to be positive.

a. $\underline{\varphi > \theta}$

The joint probability T may be decomposed into the product of a conditional and an unconditional probability

$$T(p, q, \theta, \varphi) = \overline{T}(p, q, \theta\,|\,\varphi)\, T'(p, q, \varphi)$$

(28)

where $\overline{T}(p, q, \theta\,|\,\varphi)$ is the probability that the surface does not obstruct the ray PS given that it does not obstruct PK, and $T'(p, q, \varphi)$ is the probability that the surface does not obstruct PK. $\overline{T}$ is necessarily equal to unity if $\varphi > \theta$, and T' simply $S(q, \varphi)$; thus

12

Case (a)

$$T(p, q, \theta, \varphi) = S(q, \varphi) = h(\bar{\mu} - q) \, G(\bar{\mu}) \tag{29}$$

where

$$\bar{\mu} = \cot \varphi \quad \text{and} \quad G(\bar{\mu}) = \frac{1}{\left[\Lambda(\bar{\mu}) + 1\right]}$$

b. $o < \varphi < \theta$

An exactly parallel argument to (a) in which the roles of θ and φ are interchanged leads to:

Case (b)

$$T(p, q, \theta, \varphi) = S(q, \theta) = h(\mu - q) \, G(\mu) \tag{30}$$

c. $\varphi < o$

In this case it may be assumed to a good approximation that the shadowing functions for θ and φ are independent, then T decomposes into the product:

Case (c)

$$T(p, q, \theta, \varphi) = S(q, \theta) \, S(q, \varphi)$$

$$= h(\mu - q) \, h(\bar{\mu} + q) \, G(\bar{\mu}) \tag{31}$$

Using a, b, or c the integral in equation (20) may be evaluated and for cases b and c it yields

(b)
$$f = S(\theta) \left\{ 1 - \frac{\mu}{\bar{\mu}} \right\} + \frac{\mu}{\bar{\mu}} \tag{32}$$

or

$$\frac{\left(f - \frac{\mu}{\bar{\mu}}\right)}{\left(1 - \mu/\bar{\mu}\right)} = S(\theta) \tag{33}$$

13

(c)

$$f = S(\theta)\,G(\varphi) \cdot \left[1 + \frac{\mu}{\bar{\mu}}\right] + G(\theta)\left[1 - G(\varphi)\right]$$

$$-\frac{\mu}{\bar{\mu}} \cdot G(\varphi) \tag{34}$$

If the observer views the surface away from grazing angle, $(\bar{\mu} \gtrsim w)$, $G(\bar{\mu})$ is close to unity and equation (34) becomes

$$f = S(\theta)\left\{1 + \mu/\bar{\mu}\right\} - \mu/\bar{\mu} \tag{35}$$

(a result of similar form to (32) which could equally well have been deduced by replacing $S(q,\varphi)$ by unity in the expression for $T(p, q, \theta, \varphi)$, equation (31), and

$$S(\theta) = \frac{(f + \mu/\bar{\mu})}{(1 + \mu/\bar{\mu})} \tag{36}$$

where the sign change reflects the sense of the angle of observation. If, as well, $f\bar{\mu} \gg \mu$, i.e., $|\varphi| \ll \theta$, both expressions reduce to the simple form

$$f \simeq S(\theta) \tag{37}$$

If $\theta = \varphi$, then equation (32) reduces to $f = 1$, demonstrating that

$$\iint\limits_{\text{surface}} dA\, J(p, q, \theta, \theta)\cos K\hat{P}N = A_0 \cos\theta \tag{38}$$

which expresses the self-consistency condition mentioned earlier, that the visible area of a rough surface projected onto the plane perpendicular to the direction of view is independent of the roughness and equal to the projected area of the underlying mean plane, as indeed it must be. Here lies the

14

advantage of (25) over the equivalent expression of Wagner (ref. 4). With the form of $S(q, \theta)$ derived in this paper equation (38) is satisfied identically, not approximately. The self-consistency condition also ensures that $f = 1$ for all $\varphi > \theta$, (case (a)).

The condition imposed upon the orientation of the direction of view in the plane of illumination may be relaxed at the cost of greater care in the analysis of the joint probability function $T(p, q, \theta, \varphi)$. Here attention will be restricted to the regime where equations (33, 36) are valid. On the Moon this limits observation to the equatorial region and a measurement of the shadows cast in sunlight allows, within the model, a direct determination of the mean slope of local surface roughness on the scale of resolution of the photographs used. $S(\theta)$, calculated according to equations (33, 36) from measurements of the proportion of area shadowed in atlas photographs (ref. 7) of a highland area north of Julius Caesar crater $\left[15^{\circ}E, 5^{\circ}N\right]$, is displayed in Figure 4, with theoretical curves calculated for various values of the RMS slope w. Statistical uniformity of the surface across the region examined ($\sim180 \times 180$ km^2) was assumed and the effect of varying Sun angle deduced from different north-south strips of the same photograph. Included in the diagram is a point taken from a shadow analysis in a highland region near the crater Argelander $\left[5^{\circ}E, 15^{\circ}S\right]$ made, in a different connection by Watson, Murray and Brown (ref. 8). Comparison with theory suggests a mean slope of $\sim9^{\circ}$, which if typical of large parts of the Moon compares well with the value 6° – 12° deduced from radar studies (ref. 9) for structure of greater than meter scale.

While of interest in connection with Earth-based lunar photographic studies it is suggested that shadow analysis may be useful also in estimating meter scale surface roughness from high resolution Lunar Orbiter photography which would provide a means for the rapid screening of photographs during the process of selection of a site for an Apollo landing.
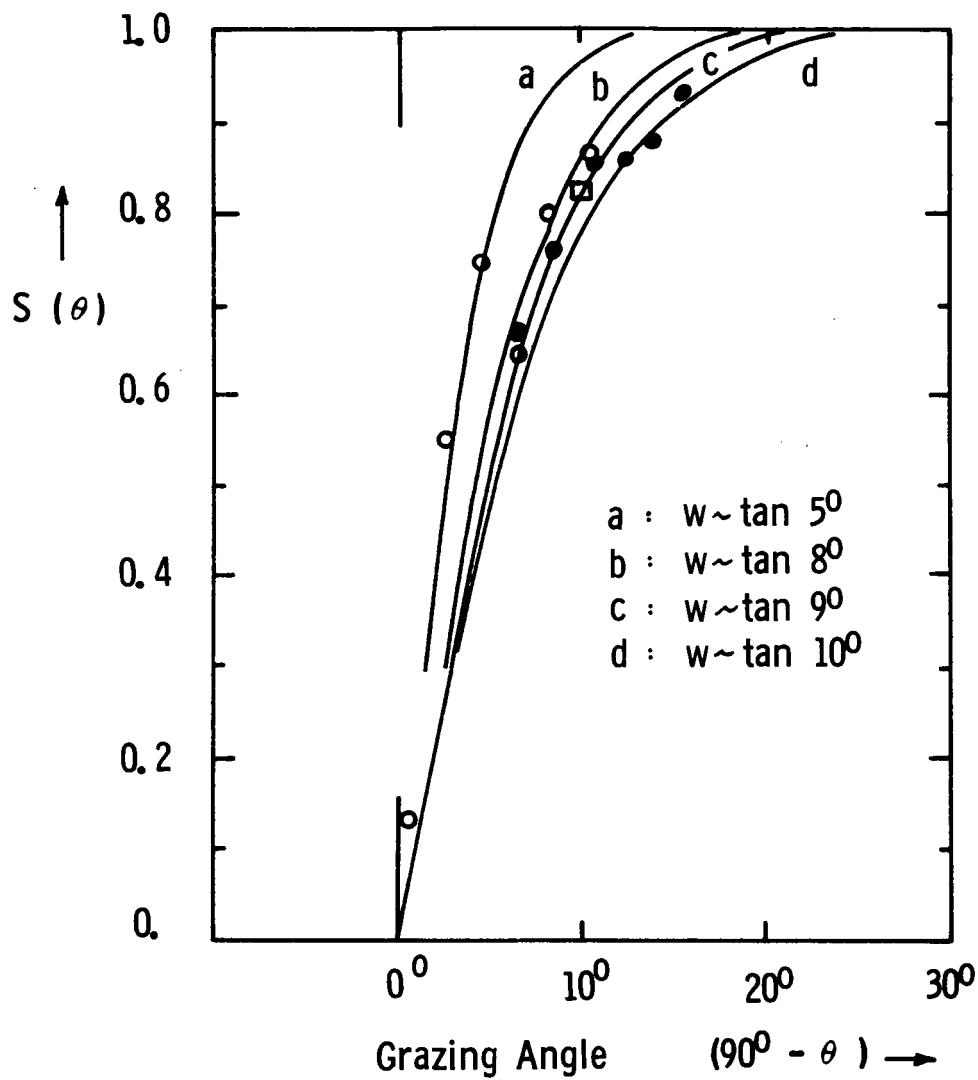
Figure 4: Shadowing function S (θ) measured from moon photographs compared with theoretical curves

INFRARED EMISSION STUDIES

Observers of the infrared emission of the Moon have noticed two pheno-
mena which are conventionally attributed to surface roughness. Pettit and
Nicholson (ref. 10), who observed the change of infrared brightness across
the equatorial belt of the full Moon disc found that the brightness decreased
as the 2/3 power of the cosine of the angle of observation rather than the
first power which would be expected for a spherical Lambertian surface.
Sinton (ref. 11), who measured the brightness of the subsolar point over a
lunation noticed an angular dependence of the brightness not given by a spher-
ical Lambertian surface. An attempt will be made to interpret both these
observations in terms of surface roughness of a scale below the resolution of
the detector.

Each surface element of the rough Moon is assumed to be a perfect Lam-
bertian emitter of thermal radiation at the wavelengths concerned. Heat flow
through the surface is neglected (a good approximation during the lunar day)
and energy balance for the surface element used to equate absorbed sunlight
with radiated thermal energy. The contribution to the radiation incident on
an element emitted or reflected by its fellows is neglected, as is any angular
dependence of the absorption coefficient. Emissive and absorptive properties
are assumed uniform across the surface, a section of which is illustrated in
Figure 5a illuminated from vertically above and observed at a distance from
the direction PK. The total energy radiated by the element δA is propor-
tional to $\delta A \cos V\hat{P}N$, and that reaching the observer proportional to

$$\delta A \cos V\hat{P}N \cos N\hat{P}K \left[J(p, q, \theta, \varphi) \right]_{\theta=0} \tag{39}$$
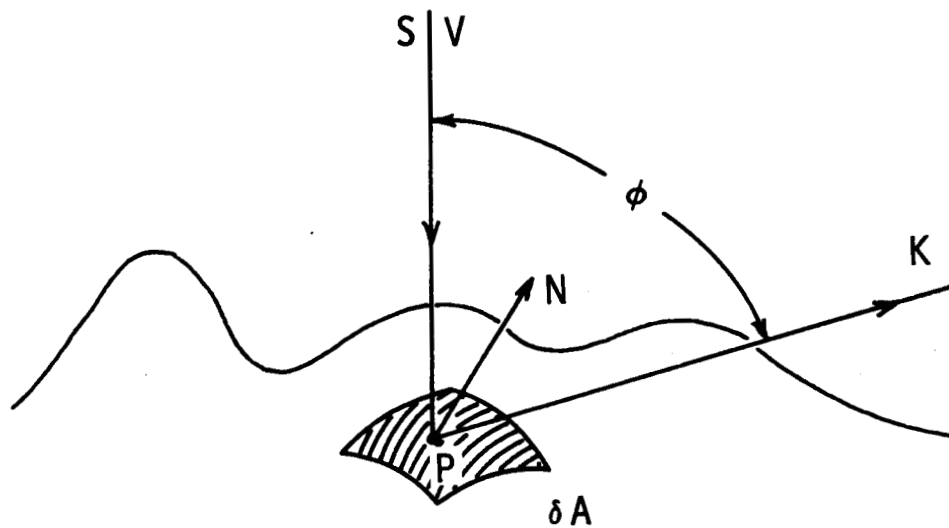
Figure 5a: Part of a random rough surface illuminated from vertically above and observed from K
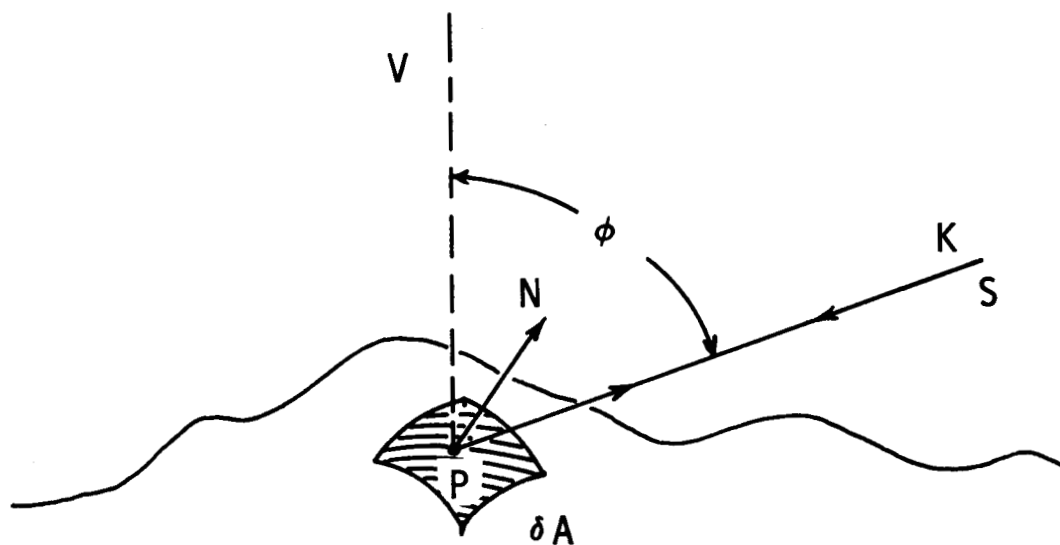

Figure 5b: Part of a random rough surface both illuminated and observed from K

The total radiation, R, reaching the observer from the surface is

$$R \propto \iint\limits_{\substack{\text{mean} \\ \text{plane}}} dxdy \; \cos N\hat{P}K \; J(p, q, 0, \varphi) \tag{40}$$

Averaging over the surface, dividing by the projected area and normalizing gives the observed brightness, $B_A(\varphi)$,

$$B_A(\varphi) = \frac{B_A(o)}{I} \iint dpdq \; P(p) \; P(q) \; \frac{[1-q \tan \varphi]}{(1+p^2+q^2)^{1/2}} \; S(q, \varphi) \tag{41}$$

where

$$\cos V\hat{P}N = \frac{1}{(1 + p^2 + q^2)^{1/2}}$$

$$\cos N\hat{P}K = \frac{\cos \varphi - q \sin \varphi}{(1 + p^2 + q^2)^{1/2}}$$

and

$$I = \int\limits_{-\infty}^{+\infty} dp \int\limits_{-\infty}^{+\infty} dq \; P(p) \; P(q) \; \frac{1}{\left[1 + p^2 + q^2\right]^{1/2}} \tag{42}$$

$B_A(\varphi)$ calculated numerically from equation (41) for various values of surface mean slope w is shown as a function of φ in Figure 6, upon which are superimposed the experimental findings of Sinton for the brightness of the subsolar point.

The change of brightness across the full Moon disc requires slightly different analysis. In Figure 5b an element of the surface is illustrated, illuminated and observed from the same angle φ. Arguments similar to those preceding equation (40) lead to an expression for the radiated energy reaching the observer from the whole surface:
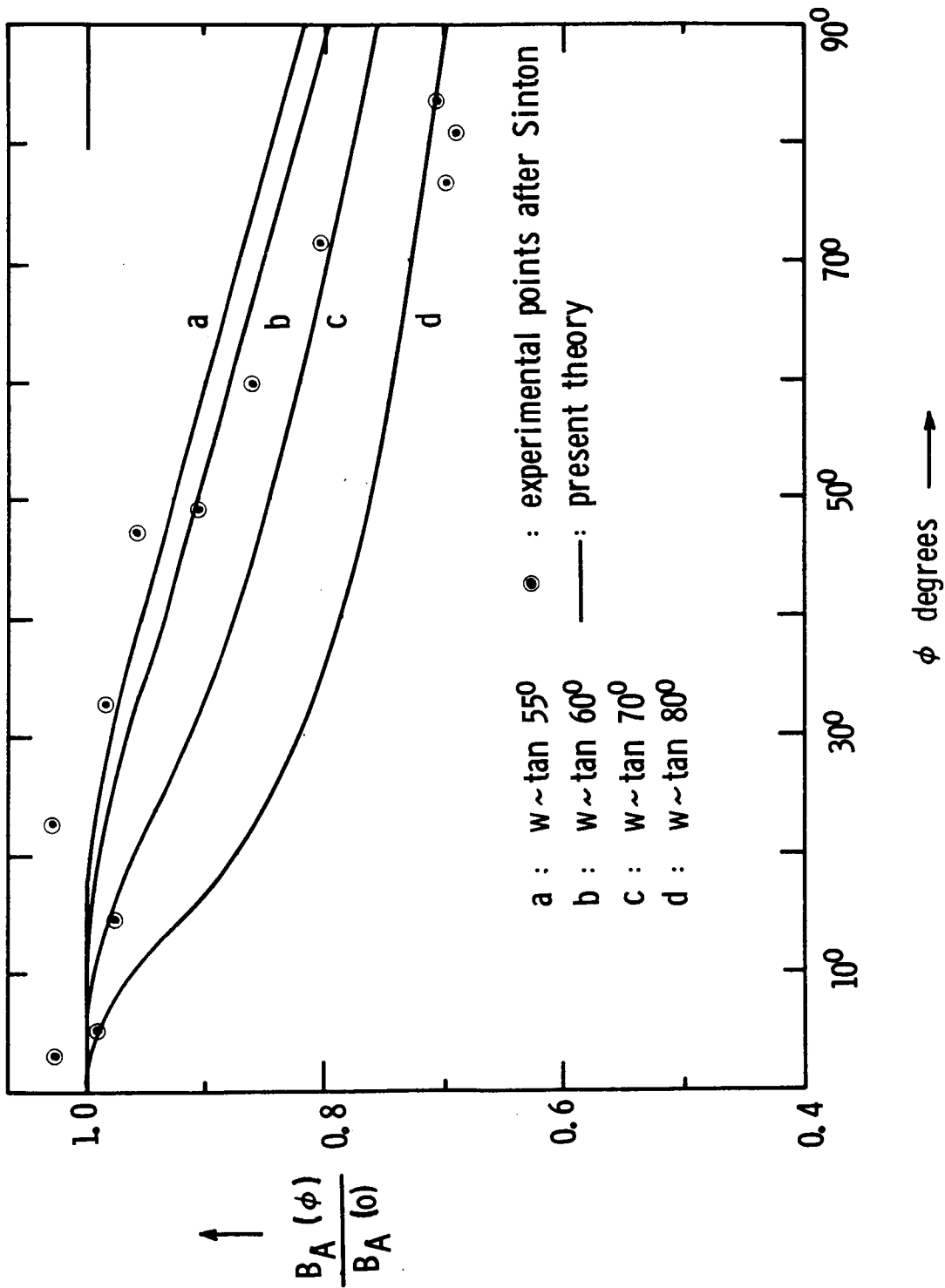
19

Figure 6: Infra red brightness variation of the subsolar point during a lunation (after Sinton) compared with theoretical curves

$$R \propto \iint_{\substack{\text{mean} \\ \text{plane}}} dxdy \ \frac{\cos^2 N\hat{P}K}{\cos V\hat{P}N} \ J(p, q, \varphi, \varphi) \tag{43}$$

The apparent brightness of the surface as a function of the angle of incidence is just

$$B_B(\varphi) = \frac{B_B(o) \cos \varphi}{I} \cdot \iint dpdq \ P(p) \ P(q) \ \frac{\left[1 - q \tan \varphi\right]^2}{(1 + p^2 + q^2)^{1/2}} \ S(q, \varphi) \tag{44}$$

Values of $B_B(\varphi)$ computed from equation (44) are displayed in Figure 7, compared with Pettit and Nicholson's experimental observations.

In each case it is seen that theory explains the qualitative features of the observations. The limbs of the full Moon disc are brighter than expected for a smooth sphere, because the collection of randomly oriented facets provides an array radiating in the direction of the observer more efficiently than the equivalent smooth surface. Conversely the subsolar point is less bright than expected, for an analogous reason.

Both $B_A(\varphi)$ and $B_B(\varphi)$ approach limits as $\varphi \rightarrow \pi/2$

$$B_A(\pi/2) = B_A(o) \ \frac{(2\pi)^{1/2}}{Iw} \ \int_{-\infty}^{+\infty} dp \int_0^{\infty} dp \ P(p) \ P(q) \ \frac{q}{\left[1 + p^2 + q^2\right]^{1/2}} \tag{45}$$
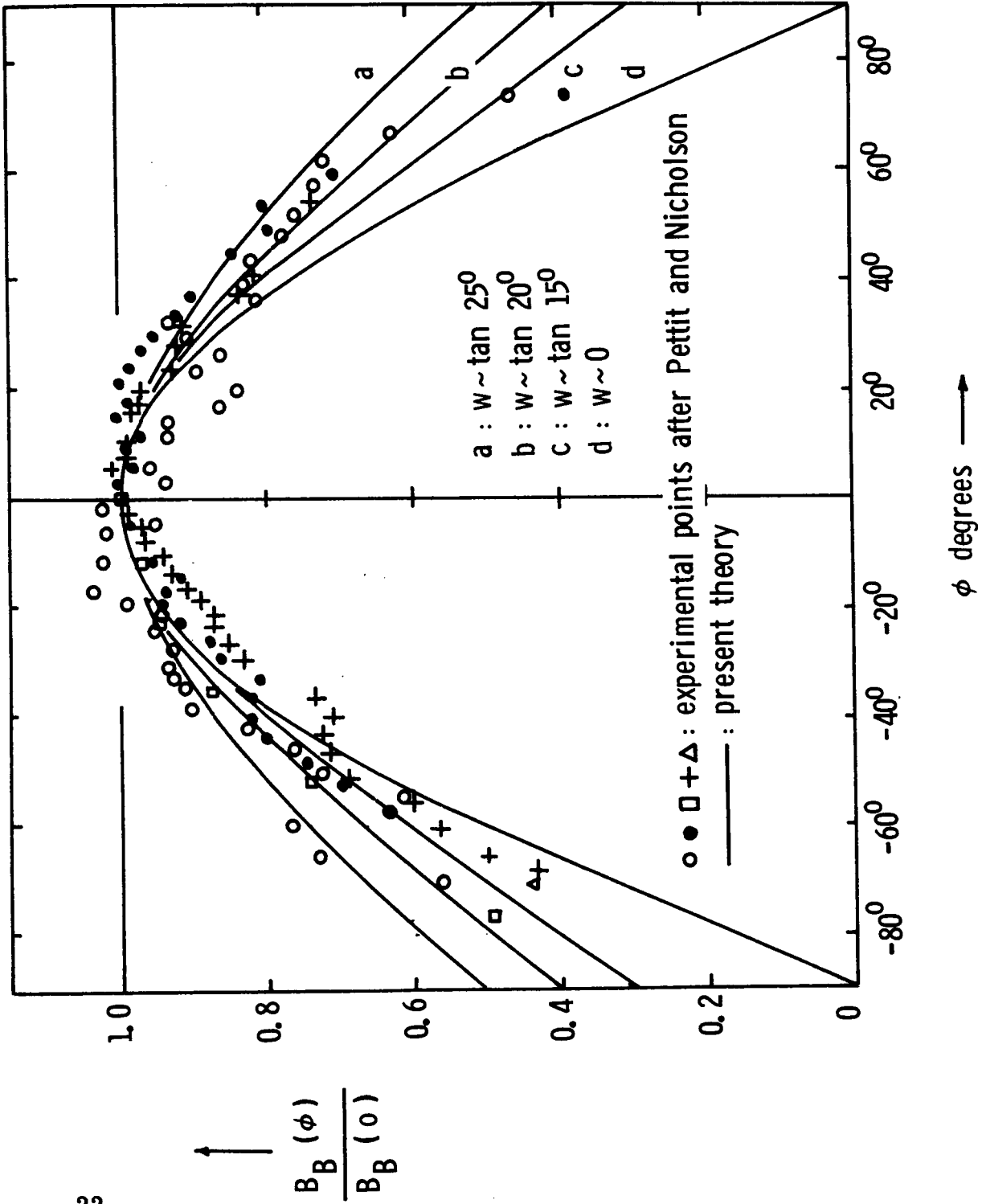
and

$$\lim_{w \rightarrow o} B_A(\pi/2) = B_A(o) \tag{46}$$

Figure 7: Infra red brightness variation across the full moon disc (after Pettit and Nicholson) compared with theoretical curves

a : w ~ tan 25⁰
b : w ~ tan 20⁰
c : w ~ tan 15⁰
d : w ~ 0

o • □ + △ : experimental points after Pettit and Nicholson
——— : present theory

ϕ degrees ——→

$\dfrac{B_B(\phi)}{B_B(0)}$

$$B_B(\pi/2) = B_B(o) \; \frac{(2\pi)^{1/2}}{Iw} \int_{-\infty}^{+\infty} dp \int_0^{\infty} dq \; P(p) \; P(q) \; \frac{q^2}{\left[1+p^2+q^2\right]^{1/2}} \qquad (47)$$

and

$$\lim_{w \to o} B_B \left(\frac{\pi}{2}\right) \sim \left[B_B(o) \cdot \left(\frac{\pi}{2}\right)^{1/2} \cdot w\right] \to o \qquad (48)$$

The quantitative agreement of theory and experiment is less satisfactory, partly because of experimental point scatter. If the model can be trusted the inference is that infra-red thermal brightness across the full Moon disc is affected primarily by structure of mean slope $\sim 20^o$, probably of large scale, but that the brightness of the subsolar point depends upon much rougher small scale structure of mean slope $60 \sim 70^o$. It is not obvious why there should be this discrepancy.

The presence of extreme roughness suggests that to describe the physical situation more closely the model should be improved to include the illumination of a facet by radiation reflected and emitted by those adjacent; as Sinton has pointed out (ref. 11) the 'valleys' will then be hotter than the 'peaks' and the apparent brightness dependent upon the proportion of each visible. In addition, a complete theory should take account of the whole range of roughness in a coherent way rather than divide structure into two classes, the one of microscopic scale responsible for producing the Lambertian behavior assumed to be characteristic of the other coarser relief, a separation made implicitly in this paper.

CONCLUSIONS

A statistical model of the Moon's surface roughness has been used in an attempt to explain the deviations of the observed gross infrared thermal emissive properties of the Moon from those characterizing a smooth Lambertian surface. Qualitative agreement is more striking than the quantitative comparison of theory and experiment, but the latter suggests that the thermal brightness variation across the full Moon disc is affected by large scale relief, of 10-20° mean slope, while variation in the brightness of the subsolar point during a lunation is determined by much rougher small scale structure. This discrepancy demonstrates a weakness of the model which might be reduced by a more careful analysis of the contribution of locally emitted radiation to the total incident energy.

The method requires development of a self shadowing theory of random rough surfaces which may be used, in a different context, to determine local mean surface slope from the amount of shadow visible in a Moon photograph. Analysis of an Earth-based photograph of a typical highland region yields 9° for the mean slope of large scale roughness. It is suggested that the technique might facilitate the rapid analysis of Lunar Orbiter photographs.

REFERENCES

1. Hopfield, J. J.: Science, 151, 1966, pp. 1380-1381.
2. Hagfors, T.: J. Geophys. Res., 69, 1964, pp. 3779-3784.
3. Middleton, D.: Introduction to Statistical Communication Theory. Chapters 7 and 8, McGraw-Hill Book Co., Inc., 1960.
4. Wagner, R. J.: TRW Systems Publication 7401-6012-R0000, June, 1966.
5. Beckmann, P.: IEEE Trans. on Antennas and Propagation, AP 13, 1965, pp. 384-388.
6. Radar Studies of the Moon. M.I.T. Lincoln Laboratory Quarterly Progress Report #2, NASA CR 76012, N66-29738, May 15, 1966.
7. Kopal, Z.: Photographic Atlas of the Moon. Plates XXXVIII and CXV, Academic Press Inc., 1965.
8. Watson, K.; Murray, B. C.; and Brown, H.: J. Geophys. Res., 66, 1961, pp. 3033-3045.
9. Evans, J. V.: Report of August, 1965 "Tycho" meeting, published by the University of Minnesota.
10. Pettit, E. and Nicholson, S. B.: Astrophys. J., 71, 1930, p. 102.
11. Sinton, W. M.: Temperatures on the Lunar Surface. In Physics and Astronomy of the Moon, ed. Z. Kopal, Academic Press, Inc., 1962.